

The effect of skew angle on the mechanical behaviour of masonry arches

V. Sarhosis*, D.V. Oliveira⁺, J.V. Lemos[#], P.B. Lourenco⁺

* School of Engineering, Cardiff University, Cardiff, UK, SarhosisV@cardiff.ac.uk

⁺ [◇]ISISE, Department of Civil Engineering, University of Minho, Portugal, danvco@civil.uminho.pt,
pbl@civil.uminho.pt

[#] National Laboratory of Civil Engineering, Lisbon, Portugal, vlemos@lnec.pt

ABSTRACT

This paper presents the development of a three dimensional computational model, based on the Discrete Element Method (DEM), which was used to investigate the effect of the angle of skew on the load carrying capacity of twenty-eight different in geometry single span stone masonry arches. Each stone of the arch was represented as a distinct block. Mortar joints were modelled as zero thickness interfaces which can open and close depending on the magnitude and direction of the stresses applied to them. The variables investigated were the arch span, the span : rise ratio and the skew angle. At each arch, a full width vertical line load was applied incrementally to the extrados at quarter span until collapse. At each load increment, the crack development and vertical deflection profile was recorded. The results compared with similar “square” (or regular) arches. From the results analysis, it was found that an increase in the angle of skew will increase the twisting behaviour of the arch and will eventually cause failure to occur at a lower load. Also, the effect of the angle of skew on the ultimate load that the masonry arch can carry is more significant for segmental arches than circular one.

Keywords: *Masonry, arches, discrete element modelling, cracking, in-plane loading.*

1 INTRODUCTION

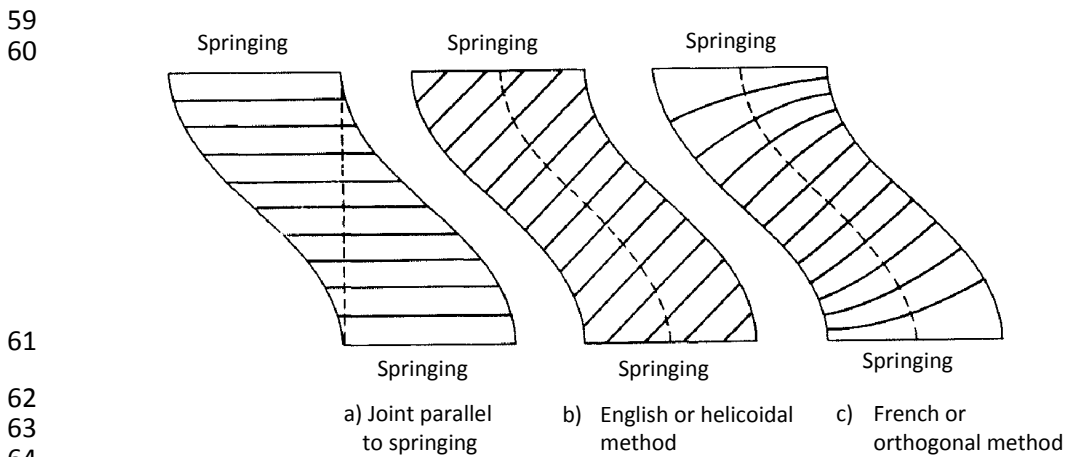
A skew arch is a method of construction that enables masonry arch bridges to span obstacles at an angle (Fig. 1). Bridges with a small amount of skew (i.e. less than 30°) can be constructed using bedding planes parallel to the abutments (Melbourne & Hodgson, 1995). However, bridges with large amount of skew present significant construction difficulties. Fig. 2 shows three well-known methods of construction for an arch spanning at 45 degrees skew (Page 1993). Fig. 2a shows the simplest form of construction where units are laid parallel to abutments. Fig. 2b shows the English (or helicoidal) method which is constructed such that the bed at the crown is perpendicular to the longitudinal axis of the bridge. For geometrical reasons and for the beds to remain parallel, the orientation of the block units causes the beds to “roll over” and thus rest on the springings at an angle (Fig. 1b). This is a cheap method of construction since every voussoir is cut similar to each other. Fig. 2c shows the French (or orthogonal) method which keeps the bed orthogonal with the local edge of the arch. This is the most expensive method of construction since it requires varying sized masonry blocks and availability of high skilled masons, since almost every block in the arch barrel to be of unique shape. The procedure used for the construction of such bridges and their mathematical curves are described in full detail by Rankine (1862).

There are many thousands of stone masonry arch bridges in Europe, many of which have spans with a varying amount of skew (Brennich & Morbiducci 2007). Most of these bridges are well over 100 years old and are supporting traffic loads many times above those originally envisaged. Different materials and methods of construction used in these bridges will influence their strength and stiffness. There is an increasing demand for a better understanding of the life expectancy of such bridges in order to inform maintenance, repair and strengthening strategies. Although a great deal of work has been carried out to assess the strength of square span masonry arch bridges using mainly two dimensional methods of analysis (Heyman 1966; Gilbert 1993; Page 1993; Melbourne & Hodgson 1995), comparatively little work has been undertaken to understand the three dimensional behaviour of skew arches (Hodgson 1996; Wang 2004). The analysis of skew arch

50 bridges has many difficulties and there is no universally accepted method of analysis yet. Today, in
 51 many countries, including UK, skew arches are routinely assessed on the basis that the skew span is
 52 straight (e.g. DB 21/01; DB16/17). However, experience from previous studies has clearly shown
 53 that depending on the methods of construction and geometry, the stiffness and strength of skew
 54 arches might be quite different (Hodgson 1996). In addition, such method is not suitable for non-
 55 standard geometries or for arches which suffered damage and deterioration.
 56



57 Fig. 1. Typical skew masonry arch constructed using the English method: (a) front view; (b) detail
 58 of the intrados



65 Fig. 2. Intrados of an arch spanning at 45° skew (Page 1993).

66 In recent years, sophisticated methods of analysis like Finite Element Method (FEM) have been
 67 applied to understand the three dimensional behaviour of arches (Choo & Gong 1995). A nice
 68 overview of the different arch models performed in the 1990's can be found in Boothby (2001).
 69 However, in such models, the description of the discontinuity is limited since they tend to focus on
 70 the continuity of the arch. Sophisticated FEM approaches (e.g. contact element techniques) are able
 71 to reflect the discrete nature of masonry. Examples of such models have been undertaken by
 72 Fanning and Boothby (2001), Gago et al. (2002), Ford et al. (2003), Drosopoulos et al. (2006). The
 73 disadvantages of these methods are mainly associated to: a) high computational cost; b) crack
 74 development cannot be obtained; and c) convergence difficulties if blocks fall or slide excessively.
 75 An alternative and appealing approach is represented by the Distinct Element Method (DEM),
 76 where the discrete nature of the masonry arch is truly incorporated. The advantage of the DEM is
 77 that considers the arch as a collection of separate voussoirs able to move and rotate to each other.
 78 The DEM was initially developed by Cundall (1971) to model blocky-rock systems and sliding
 79 along rock mass. The approach was later used to model masonry structures including arches

80 (Lemos 1995; Lemos 2007; Mirabella & Calvetti 1998; Toth 2009; Sarhosis 2014), where failure
81 occurs along mortar joints. These studies demonstrated that DEM is a suitable method to perform
82 analysis of masonry arches and to describe realistically the ultimate load and failure mechanism.
83 However, the above studies were mainly focused on the two dimensional behaviour of arches.

84 The aim of this paper is to study the three dimensional behaviour of single span skew masonry
85 arches and provide useful guidance for the design engineer. Using the three dimensional DEM
86 software 3DEC (Itasca 2004), computational models were developed to predict the serviceability
87 and ultimate state behaviour of twenty-eight stone masonry arches with different geometries and
88 skew angles. DEM is well suited for collapse analysis of stone masonry structures since: a) large
89 displacements and rotations between blocks, including their complete detachment, can be
90 simulated; b) contacts between blocks are automatically detected and updated as block motion
91 occurs; c) progressive failure associated with crack propagation can be simulated; and d)
92 interlocking can be overcome by rounding the corners.

93 At this study, arches were constructed with joints parallel to abutments (Fig. 2a). Since the
94 intention of the authors was to investigate the effect of the arch ring geometry, the effect of fill has
95 not been included at this stage. The variables investigated were the arch span, the span : rise ratio
96 and the skew angle. Results are compared against the load to cause first cracking, the magnitude of
97 collapse load, the mode of failure and the area of joints opened. The suitability of the DEM to
98 model the three dimensional behaviour of skew arches is also outlined. It is anticipated that results
99 of this study will provide insight into the structural performance of skew masonry arches as well as
100 will provide useful guidance for the design engineers.
101

102 2 OVERVIEW OF 3DEC FOR MODELLING MASONRY

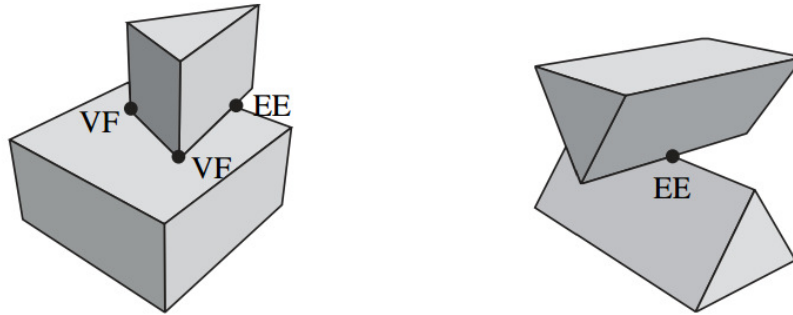
103 3DEC is an advanced numerical modelling code based on DEM for discontinuous modelling and
104 can simulate the response of discontinuous media, such as masonry, subjected to either static or
105 dynamic loading. When used to model masonry, the units (i.e. stones) are represented as an
106 assemblage of rigid or deformable blocks which may take any arbitrary geometry. Typically, rigid
107 blocks are adequate for structures with stiff, strong units, in which deformational behaviour takes
108 place at the joints. For explicit dynamic analysis, rigid block models run significantly faster. For
109 static problems, this computational advantage is less important, so deformable blocks are
110 preferable, as they provide a more elaborate representation of structural behaviour. Deformable
111 blocks, with an internal tetrahedral FE mesh, were used in the analyses reported herein. Joints are
112 represented as interfaces between blocks. These interfaces can be viewed as interactions between
113 the blocks and are governed by appropriate stress-displacement constitutive laws. These
114 interactions can be linear (e.g. spring stiffness) or non-linear functions. Interaction between blocks
115 is represented by set of point contacts, of either vertex to face or edge to edge type (Fig. 3). In
116 3DEC, finite displacements and rotations of the discrete bodies are allowed. These include
117 complete detachment between blocks and new contact generation as the calculation proceeds.
118 Contacts can open and close depending on the stresses acting on them from the application of the
119 external load. Contact forces in both the shear and normal direction are considered to be linear
120 functions of the actual penetration in shear and normal directions respectively (Itasca 2004). In the
121 normal direction, the mechanical behaviour of joints is governed by the following equation:
122

$$\Delta\sigma_n = -JK_n \cdot \Delta u_n \quad (1)$$

123 where JK_n is the normal stiffness of the contact, $\Delta\sigma_n$ is the change in normal stress and Δu_n is the
124 change in normal displacement. Similarly, in the shear direction the mechanical behaviour of
125 mortar joints is controlled by a constant shear stiffness JK_s using the following expression:
126

$$\Delta\tau_s = -JK_s \cdot \Delta u_s \quad (2)$$

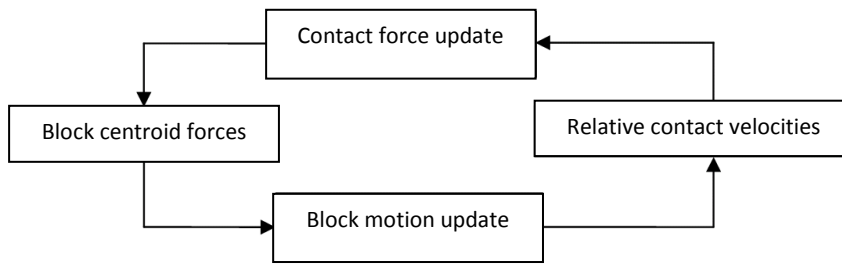
127 where $\Delta\tau_s$ is the change in shear stress and Δu_s is the change in shear displacement. These stress
128 increments are added to the previous stresses, and then the total normal and shear stresses are
129 updated to meet the selected non-elastic failure criteria, such as the Mohr-Coulomb model.



130

131 Fig. 3. Representation of block interaction by elementary vertex-face (VF) and edge-edge (EE)
 132 point contacts in 3DEC (Lemos 2007).

133 The calculations are made using the force-displacement law at all contacts and the Newton's
 134 second law of motion at all blocks. The force-displacement law is used to find contact forces from
 135 known displacements, while the Newton's second law governs the motion of the blocks resulting
 136 from the known forces acting on them. Convergence to static solutions is obtained by means of
 137 adaptive damping, as in the classical dynamic relaxation methods. Fig. 4 shows the schematic
 138 representations of the calculations taking place in 3DEC analysis.



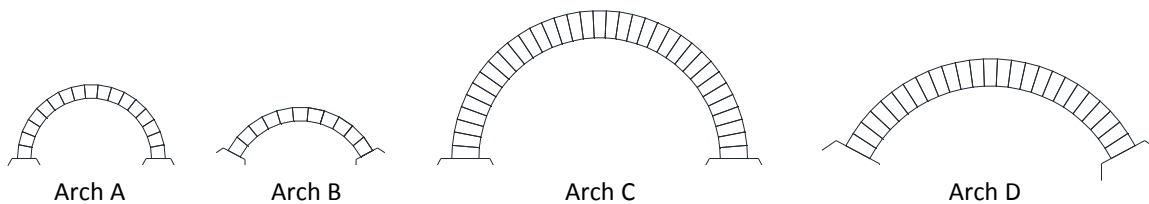
139

140 Fig. 4. Calculation cycle in 3DEC (Itasca 2004).

141 **3 COMPUTATIONAL MODELLING OF MASONRY ARCHES WITH 3DEC**

142 **3.1 Geometry**

143 Initially, geometric models of four arches have been created using 3DEC. Arches A and C had a
 144 deep semi-circular shape and Arches B and D had a semi-shallow segmental shape (Fig. 5). The
 145 semi-circular arches had the rise to span relation equal to 1:2, while the segmental arches had a
 146 lower relation and equal to 1:4. According to Jennings (2004), segmental arches are constructed
 147 where larger spans are required and gives fewer supports and lower roadway level for a given
 148 clearance under the bridge. The arch width was fixed at 4.8 m wide, which according to Oliveira et
 149 al. (2010) is typical for stone masonry arches. Geometric data of the arches used for the
 150 development of the computational models using 3DEC are shown in Table 1.



151

152 Fig. 5. Geometry of the arches studied (elevation view).

153

154

Table 1. Arch dimensions used in the analysis.

Arch	Arch shape	Skew span [m]	Rise to span ratio	Barrel thickness [m]	Width [m]
Arch A	Deep semi-circular	4.0	1:2	0.45	4.8
Arch B	Semi-shallow segmental	4.0	1:4	0.45	4.8
Arch C	Deep semi-circular	8.0	1:2	0.9	4.8
Arch D	Semi-shallow segmental	8.0	1:4	0.9	4.8

155

156 3.2 Block and interface details

157 Each stone of the arch was represented by a deformable block separated by zero thickness
 158 interfaces at each mortar joint. The deformable blocks were internally discretised into finite
 159 difference zone elements, each assumed to behave in a linear elastic manner. As failure in low
 160 strength masonry arches is predominantly at the brick/mortar joint interfaces (Melbourne &
 161 Hodgson 1995), the stresses in the stone blocks will be well below their strength limit and so no
 162 significant deformation would be expected to occur to them. The zero thickness interfaces between
 163 adjacent blocks were modelled using the elastic perfectly plastic coulomb slip failure criterion with
 164 a tension cut-off. This means that, if in any of the numerical calculations the value of tensile bond
 165 strength or shear strength is reached at a certain location, then the tensile strength and cohesion are
 166 reduced to zero at that location (Itasca 2004). Material parameters for the stone blocks and the
 167 mortar joints have been obtained from the literature (Lemos 2007; Toth 2009) and presented in
 168 Table 2 and Table 3.

169

Table 2. Properties of the masonry units.

Density [kg/m ³]	Young Modulus [N/m ²]	Poisson's ratio [-]	Bulk Modulus [N/m ²]	Shear Modulus [N/m ²]
2700	50E9	0.2	27.7E9	20.8E9

170

Table 3. Properties of the interfaces.

Joint Normal Stiffness [N/m ³]	Joint Shear Stiffness [N/m ³]	Joint Friction Angle [Degrees]	Joint Tensile Strength [N/m ²]	Joint Cohesive Strength [N/m ²]	Joint Dilatation Angle [Degrees]
7.64E9	1.79E9	35	0.1E6	0.1E6	0

171

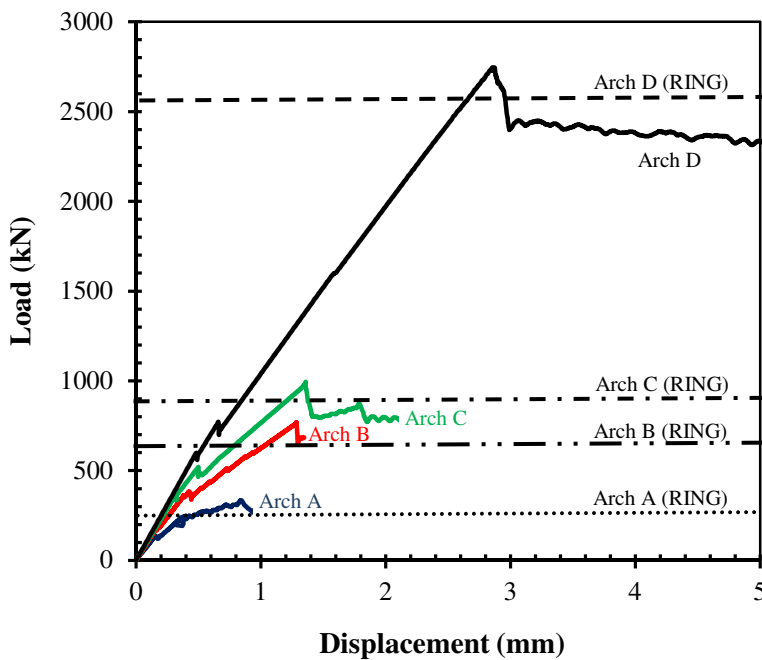
172 3.3 Boundary conditions and loading

173 Since the intention of the authors was to investigate the effect of the arch ring geometry, the
 174 abutments of the arch were modelled as rigid supports in the vertical and horizontal directions. The
 175 local damping option was selected for the static analysis algorithm.

176 Self-weight effects were assigned as a gravitational load. Gravitational forces cause the raise of
 177 compressive forces within the blocks of the arch and result in the stabilisation of the arch. Initially,
 178 the model was brought into equilibrium under its own self weight. An external full width
 179 descending linear load was applied incrementally on the arch at one quarter of the span parallel to
 180 the abutments until the arch collapsed. The loading history was imposed by applying a velocity at
 181 the loading block. In order to determine the applied load at each time-step, a subroutine has been
 182 written using FISH (an embedded language in 3DEC) which was able to trace the reaction forces
 183 from the fixed velocity grid points acting on the loading block. Evolution of the displacement of
 184 the block below the loading point was recorded. This was later used to obtain load-displacement
 185 relationships.

186 **3.4 Validation of the computational model**

187 The reliability of the numerical model evaluated by comparing the ultimate load obtained from
188 3DEC against those obtained by imposing the limit equilibrium of the arch at collapse using the
189 two dimensional limit analysis software RING 2.0 (LimitState 2009). Since RING is a two
190 dimensional software, comparisons were made with respect to the four square span arches (i.e. zero
191 skew). Also, for this comparative study and with the assumption that the limit analysis theorem
192 applies (Heyman 1966), the tensile and cohesive strength of the interfaces in 3DEC model have
193 been assumed to be equal to zero. The comparisons between the numerical and analytical results,
194 for the four square arches, are shown in Fig. 6. The little peaks in the curves shown in Fig. 6
195 represent relaxation of the loading and moment redistribution in the arch due to the formation of a
196 new crack. When a crack propagates there is an abrupt loss in stiffness in the arch. Good
197 correlation was obtained between the results from the limit analysis and the 3DEC model.



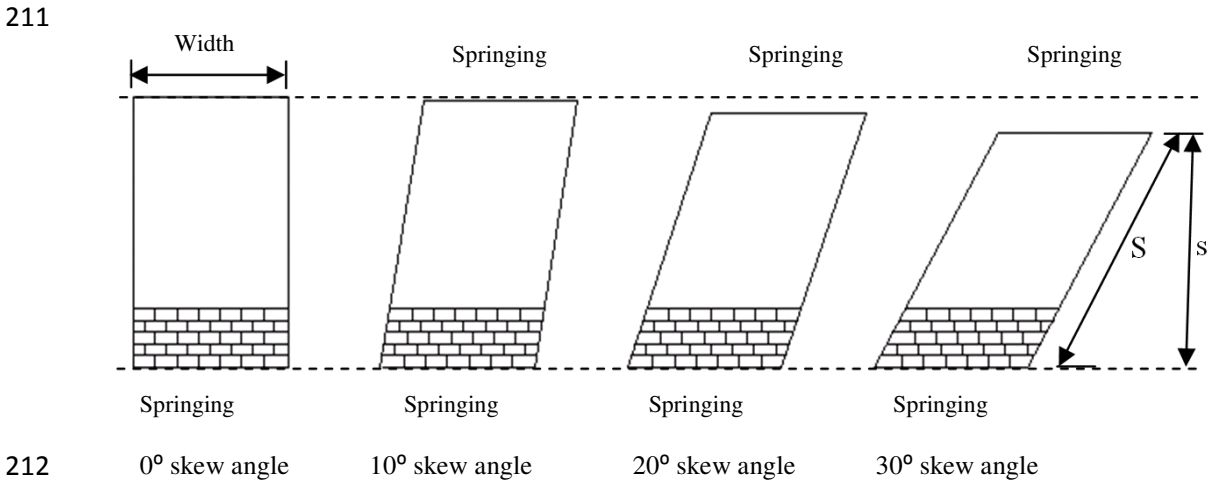
198
199 Fig. 6. Load against displacement relationship for the four square (i.e. zero skew) arches studied.

200
201 **4. PARAMETRIC ANALYSIS**

202 **4.1 Influence of the angle of skew**

203 The influence of the angle of skew is investigated by comparing square arches against those with
204 different angles of skew with respect to the load at first crack, mode of failure, load carrying
205 capacity and area of joint opened. All arches were constructed with joints parallel to springing.
206 According to Melbourne & Hodgson (1995), this type of construction is found to arches with small
207 angles of skew. For this reason, the angle of skew (φ) was varied from 0 to 30 degrees with 5
208 degrees interval. Also, the span (S) parallel to the axis of the arch has been kept constant for all

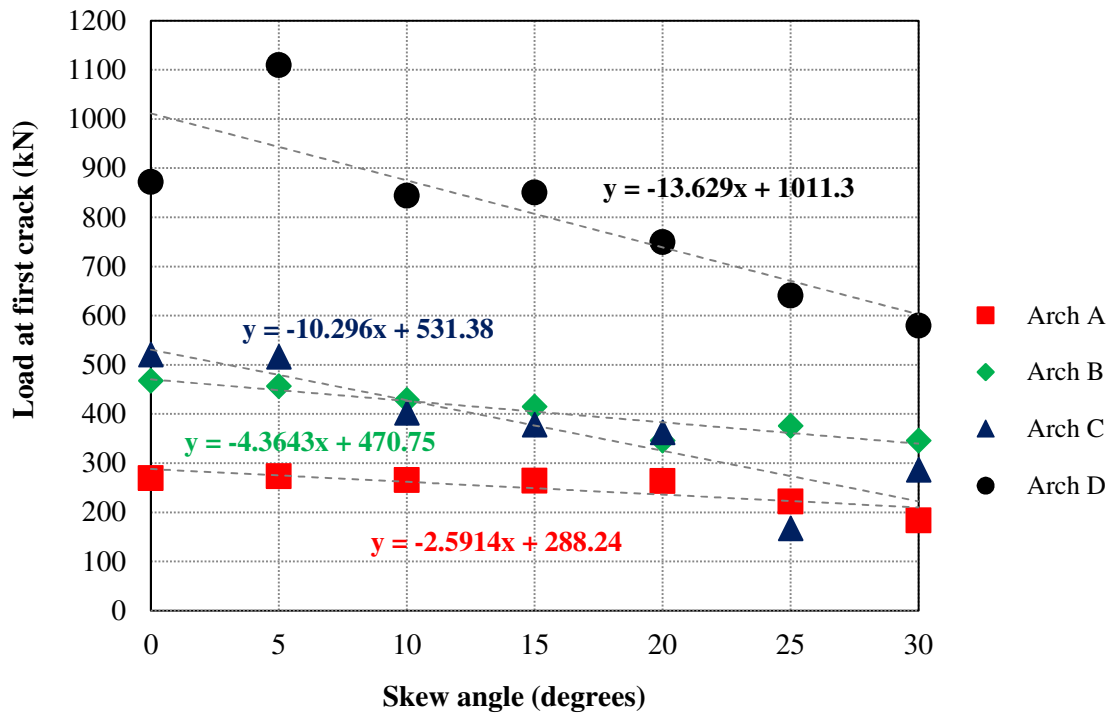
209 arches. As a result, the square span (s) of the arches decreased as the angle of skew (ϕ) increased
 210 (Fig. 7). The square span of each arch was equal to $s = S \times \cos(\phi)$.



213 Fig. 7. Geometry of the arches studied: Plan view of a typical arch.

214 **4.2 Load at first crack**

215 Cracks in masonry may not open uniformly but may open and close according to the variation of the
 216 stress field over a period of time. In 3DEC, a contact point is defined as “open” if there is currently on
 217 the contact a zero normal force. For the purpose of this study, a FISH function has been written that
 218 was able to trace contact opening greater than 0.2 mm. Usually, cracks of 0.2 mm and wider are
 219 assumed to be significant because they are visible to the naked eye. The load required to cause crack
 220 opening of 0.2 mm for each of the arches modelled with 3DEC is shown in Fig. 8. From Fig. 8, for all
 221 of the arches studied, the load at which first cracking occurs linearly decreases as the angle of skew
 222 increases.



223

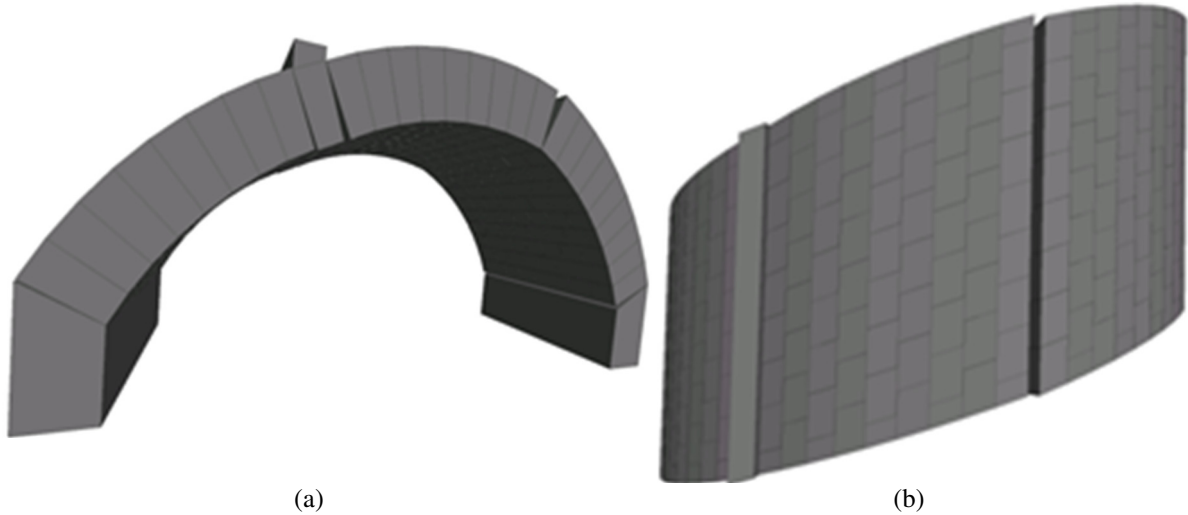
224

Fig. 8. Variation of load to cause first crack with change in skew angle.

225

226 4.3 Cracking

227 The initiation and propagation of cracks under increasing applied load have been simulated. Each
228 arch failed by the development of a four hinge mechanism (Fig. 9). Due to the line loading which
229 was applied in the arches, the hinge lines developed where parallel to the abutments. This was
230 possibly facilitated by the effect of the stiff abutments. Similar findings have also been reported by
231 Abdunur (1995). The failure mode of the Arch D with a 20 degrees angle of skew shown in Fig. 9.
232



233

234 Fig. 9. Failure mode of the Arch D with 20 degrees angle of skew: (a) front view; (b) plan
235 view.
236

236

237 4.4 Ultimate load

238 The magnitude of the ultimate load that each of the studied arches can carry is presented in Fig. 10.
239 From the results analysis, the ultimate load decreases linearly as the angle of skew increases from
240 0° to 30°. Similar trends were also reported by Melbourne (1995). The absolute decrease in
241 ultimate load due to skew is more significant for the arches with longer span and higher load
242 capacity. Also, from Fig. 10, segmental arches can carry almost two times more load than the
243 circular ones. The effect of barrel thickness and span has an effect on the load carrying capacity.
244 By doubling the barrel thickness and span, the arch can sustain approximately three times more
245 load.

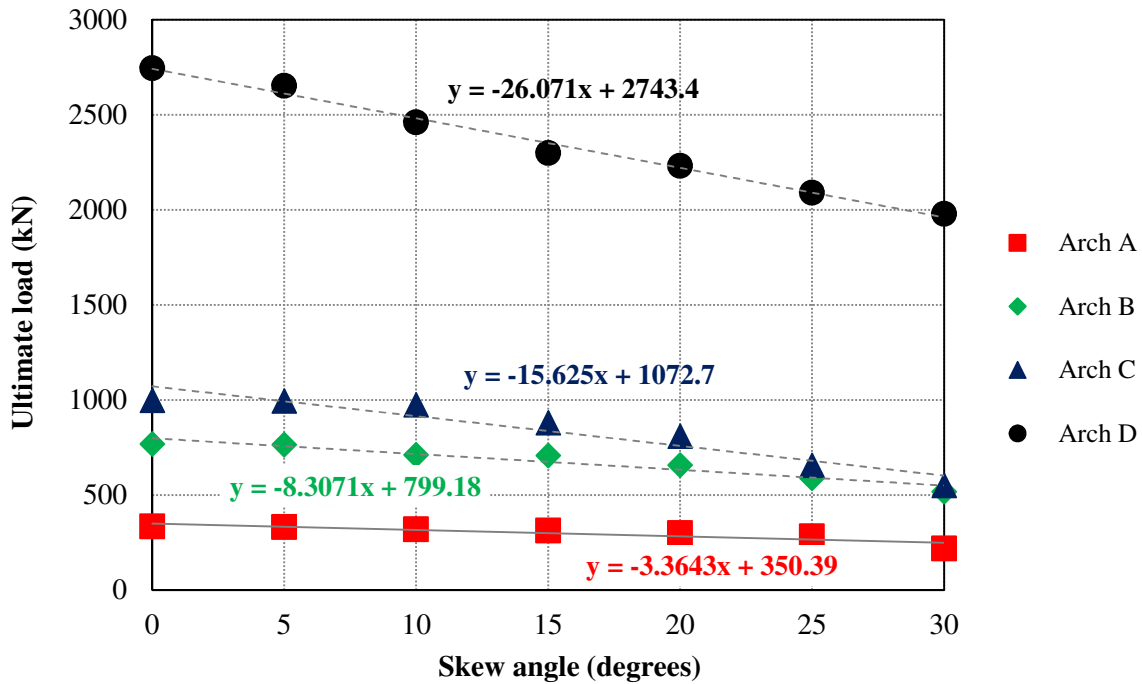
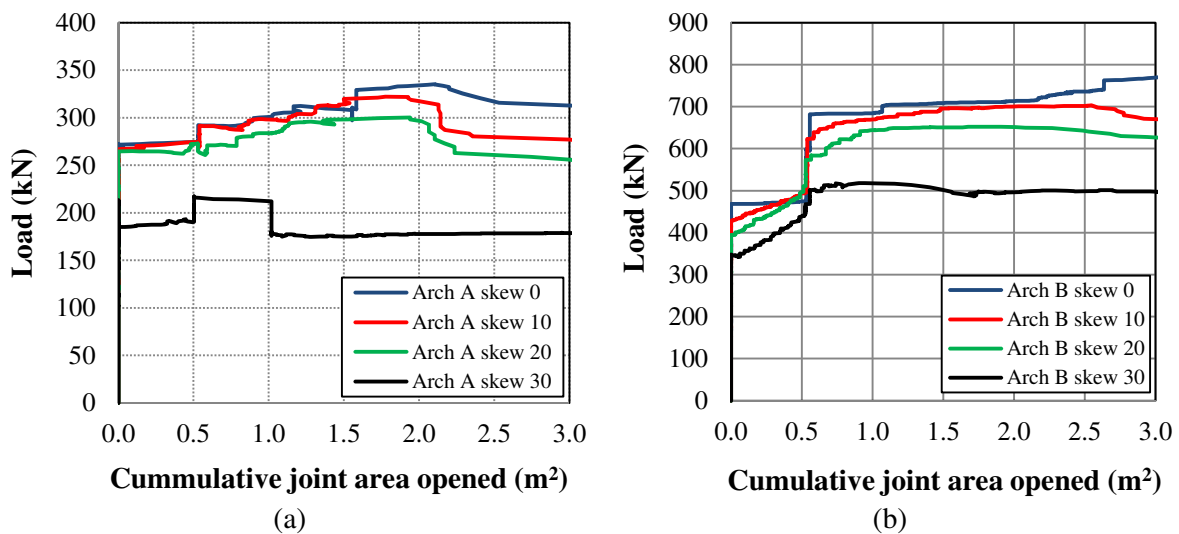
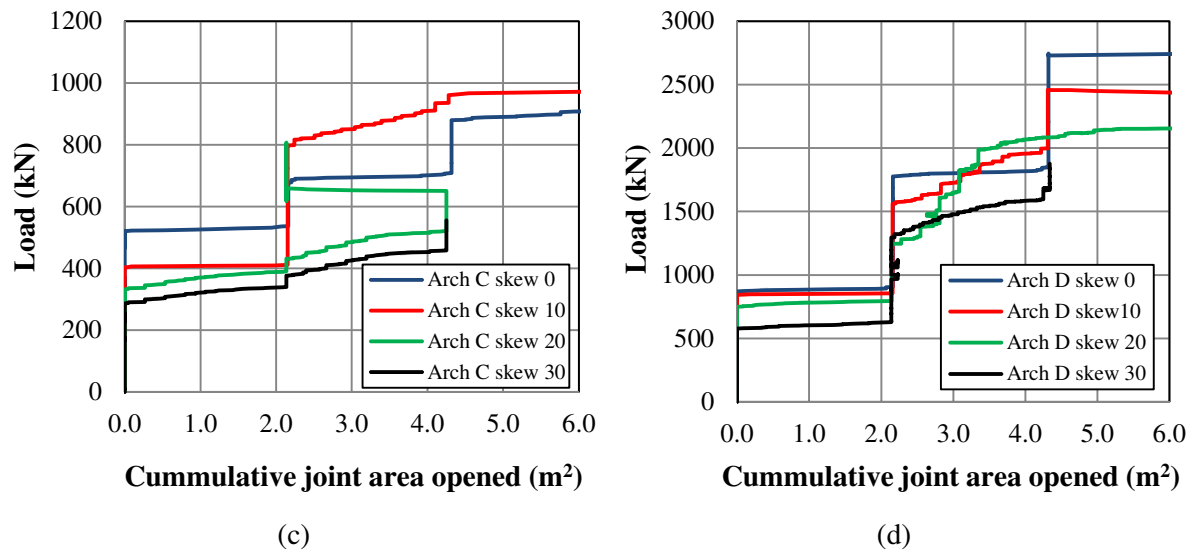


Fig. 10. Variation of ultimate load with change in skew angle.

4.5 Influence of the angle of skew on the total area of joints opened.

The increase of joint opening in the masonry arch, with the application of external load, relates to the accumulation of damage. The effect of skew on the total area of joints opened in the arch for each load increment has investigated. The cumulated area of joints opened has been calculated using a FISH function in which a joint defined as “open” when the normal force at this area is equal to zero and an opening equal or greater to 0.2 mm occurs. Fig. 12 shows the relations between the cumulative area of joints opened with the application of load for all of the arches studied. From Fig. 12, as the angle of skew increases, joint opening starts at lower loads, and for the same application of load, the cumulative area of joints opened increases.





258 Fig. 12. Variation of the cumulative joint area opened with load for the arches studied.

259 6 CONCLUSIONS

260 The Discrete Element Method in the form of the 3DEC software has been used to investigate the
 261 effect of the angle of skew on the load carrying capacity of twenty eight single span stone masonry
 262 arches. A full width linear increasing load was applied to the extrados of the arch at quarter span
 263 until collapse. The load at first cracking, the mode of failure, the ultimate load that the arch can
 264 carry and the area of joints opened with the application of load were recorded. The main
 265 conclusions that can be made based on the above study are:

- 266 a) In order to capture the complex geometry and behaviour of skew arches, it is necessary to
 267 make use of three dimensional computational models;
- 268 b) 3DEC was able to relate the evolution of load with the progressive development of hinges;
- 269 c) Each arch barrel failed by the development of a four-hinge mechanism. In some cases,
 270 hinges developed parallel to the abutments;
- 271 d) The simulations of the ultimate load indicated that an increase in the angle of skew will
 272 increase the twisting behaviour of the arch and will eventually cause failure to occur at a
 273 lower load;
- 274 e) The ratio between the load at first cracking and the ultimate load depends on the geometry of
 275 the arch and ranges from 0.3 (Arch D) to 0.9 (Arch A);
- 276 f) The effect of the angle of skew on the ultimate load that the arch can carry is more
 277 significant for segmental arches than circular one;
- 278 g) Variations in the span and rise: span ratios have an effect on the strength of the arch bridges;
- 279 h) For the same application of load, the cumulative area of joints opened increases as the angle
 280 of skew increases.

281 For the purpose of this study, arches were assumed to be constructed with the joints parallel to the
 282 springing. Further studies are required to investigate the influence of construction method to the
 283 mechanical behaviour of the arch, as well as the effect of the fill material.

284 **REFERENCES**

- 285 Abdunur, C., 1995. Direct assessment and monitoring of stresses and mechanical properties in
286 masonry arch bridges. Arch Bridges. Thomas Telford, London.
287
- 288 Boothby, T.E., 2001. Analysis of masonry arches and vaults. Progress Structural Engineering
289 Materials. 3, 246-256.
290
- 291 Brencich, A., Morbiducci, R., 2007. Masonry arches: Historical rules and modern mechanics.
292 International Journal Architectural Heritage. 1(2), 165–189.
293
- 294 Choo, B.S., Gong, N.G., 1995. Effect of skew on the strength of the masonry arch bridges. In Arch
295 Brides: Proceedings of the First International Conference of Arch Bridges. 205-214. London:
296 Thomas Telford.
297
- 298 Cundall, P.A., 1971. A computer model for simulating progressive large scale movements in
299 blocky rock systems. In: International Society of Rock Mechanics; Proc. Intern. Symp., Nancy,
300 France.
301
- 302 Department of Transport, 1993. The assessment of highway bridges and structures, Note, BA16/93.
303
- 304 Design Manual for Roads and Bridges (DMRB), 2001. Highway structures: Inspection and
305 maintenance. Assessment of highway bridges and structures. DB 21/01. London: Highway Agency.
306
- 307 Design Manual for Roads and Bridges (DMRB), 2001. Highway structures: Inspection and
308 maintenance. Assessment of highway bridges and structures. DB 16/17. London: Highway Agency.
309
- 310 Drosopoulos, G.A., Stavroulakis, G.E., Massalas, C.V., 2006. Limit analysis of a single span
311 masonry bridge with unilateral frictional contact interfaces. Engineering Structures. 28, 1864–1873.
312
- 313 Gago, A., Alfaiate, J., Gallardo, A., 2002. Numerical analyses of the Bargower arch bridge. In:
314 Finite Elements in Civil Engineering Applications: Proceedings of the Third Diana World
315 Conference, Tokyo, Japan, 9–11 October.
316
- 317 Gilbert, M., 1993. The behaviour of masonry arch bridges containing defects. PhD thesis. UK:
318 Manchester University.
319
- 320 Fanning, P.J., Boothby, T.E., 2001. Three-dimensional modelling and full-scale testing of stone
321 arch bridges. Computer & Structures. 79, 2645–2662.
322
- 323 Ford, T.E., Augarde, D.E., Tuxford, S.S., 2003. Modelling masonry arch bridges using commercial
324 finite element software. In: 9th International Conference on Civil and Structural Engineering
325 Computing, Egmond aan Zee, The Netherlands, 2–4 September
326
- 327 Henry A., 1986. Test on masonry arch bridge at Bargower, Department of Transport, TRRL
328 contractor report 7, Crowthorne, UK.
329
- 330 Heyman, J., 1966. The stone skeleton. International Journal of Solids and Structures. 2(2), 249-256.
331
- 332 Hodgson, J. 1996. The behaviour of skewed masonry arches. PhD thesis. UK: University of
333 Salford.
334
- 335 Itasca, 2004. 3DEC – Universal Distinct Element Code Manual. Theory and Background.
336 Minneapolis: Itasca Consulting Group.
337

338 LimitState, 2009. RING: Theory and modelling guide. LimitState, Sheffield.
339
340 Lemos, J.V., 1995. Assessment of the ultimate load of a masonry arch using discrete elements.
341 Computer Methods in Structural Masonry – 3, J. Middleton & G.N. Pande Ed., Swansea, UK:
342 Books & Journals International.
343
344 Lemos, J.V., 2007. Discrete element modelling of structures. *International Journal of Architectural*
345 *Heritage* 1(2):190-213.
346
347 Melbourne, C., Hodgson, J.A., 1995. The behaviour of skewed brickwork arch bridges. In *Arch*
348 *Bridges: Proceedings of the First International Conference of Arch Bridges*: 309-320. London:
349 Thomas Telford.
350
351 Mirabella, R.G. & Calvetti, E. 1998. Distinct element analysis of stone arches. In Sinopoli (ed.),
352 Arch Bridges; Proc. intern. symp., Paris, 6-9 October 1998. Rotterdam: Balkema.
353
354 Oliveira, D.V., Lourenço, P.B. & Lemos, C. 2010. Geometric properties and ultimate load carrying
355 capacity of masonry arch bridges from the Northwest Iberian Peninsula. *Engineering Structures* 32:
356 3955-3965.
357
358 Page, J., 1989. Load tests to collapse on two arch bridges at Strahmashie and Barlae, TRRL
359 research report 201, Crowthorne, UK.
360
361 Page, J., 1987. Load tests on collapse in two arch bridges at Preston, Shropshire and Prestwood,
362 Staffordshire, Department of Transport TRRL research report 110, Crowthorne, UK.
363
364 Page, J., 1993. Masonry Arch bridges, *TRL State of the Art Review*. London: HMSO.
365
366 Rankine, W.J.M., 1862. A manual for Civil Engineering. London:C. Griffin and Co.
367
368 Sarhosis, V., Sheng, Y., 2014. Identification of material parameters for low bond strength
369 masonry, *Engineering Structures* , 60, 100-110
370
371 Toth, A.R., Orban, Z., Bagi, K., 2009. Discrete element modelling of a stone masonry arch.
372 *Mechanics Research Communications*. 36(4), 469-480.
373
374 Wang, J., 2004. The three dimensional behaviour of masonry arches. PhD thesis. UK: University of
375 Salford.